polymer papers

The mobility of ethyl acetate in poly(vinylidene fluoride): rheo-photoacoustic Fourier transform infra-red studies

Bret W. Ludwig and Marek W. Urban*
Department of Polymers and Coatings, North Dakota State University, Fargo, ND 58015, USA
(Received 24 May 1991; revised 11 September 1991; accepted 25 October 1991)

The rate of diffusion of ethyl acetate (EtAc) in poly(vinylidene fluoride) (PVF_2) has been monitored using a newly developed rheo-photoacoustic Fourier transform infra-red technique. The rate depends on the degree of applied strain, the structural changes occurring during the polymer plastic deformation, the concentration of EtAc in PVF_2 as well as the morphology of the polymer. These relationships are discussed in terms of the fractional free volume (FFV) theory of transport properties in polymers. The data indicate that for larger FFV, the rate of diffusion increases. Furthermore, the elongations at which plastic strain reaches a maximum, the changes that occur during plastic deformation and the difference between relaxed and non-relaxed plastically deformed films can be determined using specially designed rheo-photoacoustic Fourier transform infra-red apparatus.

(Keywords: diffusion; ethyl acetate; poly(vinylidene fluoride); rheo-photoacoustic; Fourier transform)

INTRODUCTION

When a polymer film undergoes elongation, the morphology and transport properties change. While morphological changes can be qualitatively determined by optical and electron microscopy[1], transport properties are usually represented by two independent quantities: sorption (S), defined as the equilibrium concentration of sorbate per gram of dry polymer; and the diffusion coefficient (D), a measure of the sorbate mobility in the polymer. The product of S and D is referred to as the permeability of the system.

One of the major factors influencing sorption and diffusion of small molecules in polymer networks is the fractional free volume (FFV)[2,3] of the amorphous component of the film. It is commonly described as a measure of the probability of creating a sorption site. The latter is often visualized as a hole in the film which may be occupied by diffusant molecules. FFV should not be thought of, however, as an actual distribution of voids within the film[3]. For amorphous polymers, FFV will not change upon elongation as long as the specific volume of the polymer remains constant[4] and the amorphous network does not crystallize.

The situation will be different, however, when crystalline structures are present in a polymer network because according to previous studies[4,5], the presence of crystalline structures has a significant effect on the transport properties in polymers. The crystallites are usually considered to be impermeable to the diffusing gases or vapours, and are represented as physical crosslinks of high functionality that make up larger crystalline regions referred to as spherulites. The amorphous phase fills the space between spherulites to form a semicrystalline polymer network. The phases are intimately connected to each other through amorphous phase molecules with one or both ends contained in adjacent crystals.

When small molecules are introduced to the polymer system containing crystalline and amorphous regions, they most likely remain in the amorphous component and, in order to retain mobility, they usually follow a relatively lengthy path around the crystals. As a result, the values of diffusion coefficients for semicrystalline polymers (D_c) are in general lower than those for the corresponding pure amorphous networks (D_a). Thus, in an effort to account for the presence of crystallites, the diffusion coefficients of semicrystalline polymers are corrected through the relationship between D_c and D_a:

$$D_c = \psi D_a \qquad (1)$$

where ψ is the tortuosity factor[2].

While external forces imposed on amorphous networks do not significantly affect diffusion properties because the specific volume of the polymer remains essentially unchanged, the situation is different for highly crystalline and semicrystalline polymers. When external forces are applied to semicrystalline polymers, the interaction of the tie molecules with the crystals inhibits lateral contraction. As crystallites are drawn apart, the amorphous regions widen and their volume increases, giving rise to an increase of FFV. This behaviour, in turn, leads to the enhancement of transport properties through the network[2,3]. Stresses imposed on polymers are therefore important because after application of stress, there are two types of strains in polymers. An

---

*To whom correspondence should be addressed

0032-3861/92/163343-08

elastic strain, which increases the specific volume of the polymer, and therefore the FFV of the amorphous phase, and plastic strain, which does not affect the polymer specific volume. The magnitude of the plastic strain depends upon the relaxation time after drawing, the presence and concentration of plasticizing agents, the degree of elongation and temperature[2].

At higher elongations, when small molecules diffuse through the semicrystalline polymer, the diffusion coefficient may be decreased by the formation of a microfibrillar structure. The spherulitic structures present in the film may be destroyed, and the crystallites may line up to form microfibrils. Tie molecules stretched tightly between the crystallites compress the amorphous phase, causing a decrease of the FFV and permeability of the polymer[6].

However, it should be realized that the FFV of the network, and therefore transport properties, can also be increased by the addition of a low molecular weight permeant to the polymer. The permeant molecules, often referred to as plasticizers, swell the polymer and increase the freedom of motion of the polymer chains by disturbing interactions between them. Additional volume due to swelling and the increased mobility of the polymer molecules result in the increase of both the rates of diffusion and sorption. In fact, for the majority of polymers, the diffusion coefficient increases exponentially with the concentration of permeant[7].

With these considerations in mind, let us consider a poly(vinylidene fluoride) (PVF_2) network and examine the behaviour of relatively small ethyl acetate (EtAc) molecules migrating through this polymer. Mobility of EtAc in PVF_2, which may exist in four different crystalline forms (α, β, γ and δ), is of particular interest because EtAc is known[8] to plasticize PVF_2. Furthermore, when PVF_2 is elongated, the monoclinic α phase undergoes transformation to the orthorhombic β phase[9,10]. These phase transformations accompany the changes of the film morphology from spherulitic to fibrillar structures[1], resulting in a modification of transport properties of the polymer. Because transport properties in particular have been recognized as a means of determining polymer morphology to further understand structures and structural changes that occur during the uniaxial strain, in this study we will focus on monitoring the mobility and diffusion of EtAc in the α and β phases of PVF_2 using photoacoustic Fourier transform infra-red (*FT*i.r.) spectroscopy. If indeed the structural changes occurring during deformations of PVF_2 are related to the mobility of EtAc in PVF_2, diffusion of EtAc will provide a means of monitoring elastic and plastic elongations. For that purpose, the newly developed rheo-photoacoustic (RPA) *FT*i.r. spectroscopic approach will be used[11,12]. Although there were reports dealing with diffusion in polymers that utilized transmission *FT*i.r. spectroscopy[13], RPA *FT*i.r. is capable of physically isolating the spectra of sorbate molecules present in the polymer network and in the gas phase above the polymer surface. To the best of our knowledge, this is the first study of diffusion in polymers using the RPA *FT*i.r. approach.

EXPERIMENTAL

Sample preparation

PVF_2 films (150 μm thick) were obtained from Westlake Co. The films were cut to size (~7.6 cm × 1.3 cm) and EtAc was introduced to the film specimens by soaking them in pure EtAc for a minimum of 1 week. The samples were allowed to dry for various amounts of time at ambient temperature and pressure before being loaded into the RPA *FT*i.r. cell.

RPA FT*i.r. and X-ray measurements*

All RPA *FT*i.r. spectra were recorded using a Digilab FTS-10 spectrometer equipped with a specially designed RPA cell[14]. Each spectrum was obtained by collecting 400 co-added scans at a resolution of 4 cm^{-1} and ratioed against a carbon black reference. A detailed description of the cell has been provided elsewhere[14]. Unless otherwise stated, RPA *FT*i.r. experiments involve the use of the photoacoustic 'umbrella' recently developed in our laboratory[15]. The experiments were performed on PVF_2 films shielded from the i.r. beam with aluminium foil (*Figure 1*). Such an arrangement allows only gaseous EtAc to be 'seen' by the i.r. source and to be detected by a photoacoustic microphone. *Figure 2* shows two spectra for the PVF_2 film (α phase) and the EtAc vapour. Because the most convenient spectral feature in EtAc is the carbonyl band at 1768 cm^{-1}, this band will be employed in the forthcoming analysis of diffusion in PVF_2.

In these studies, three series of experiments were conducted. The first involved loading the sample into the

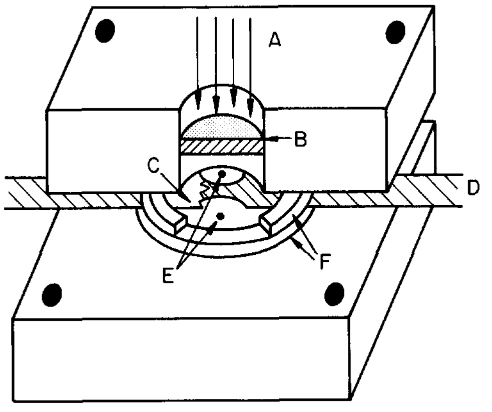

Figure 1 Schematic diagram of the sample compartment of the RPA *FT*i.r. cell: (A) incident i.r. beam; (B) KBr window; (C) aluminium foil; (D) sample; (E) helium inlet and outlet; (F) rubber O-rings

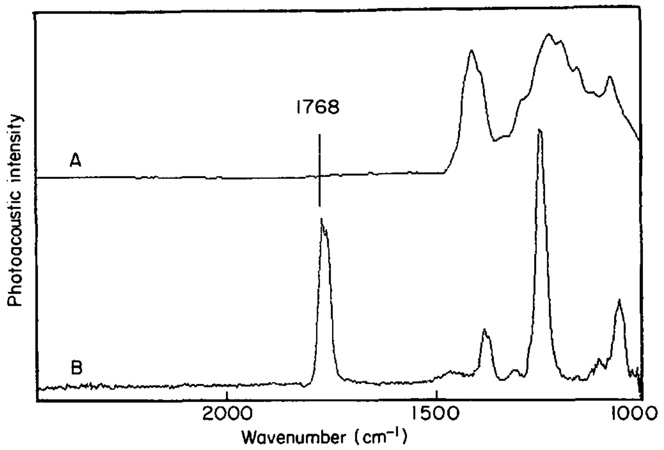

Figure 2 RPA *FT*i.r. spectra of (A) PVF_2 film (α phase) and (B) EtAc vapour

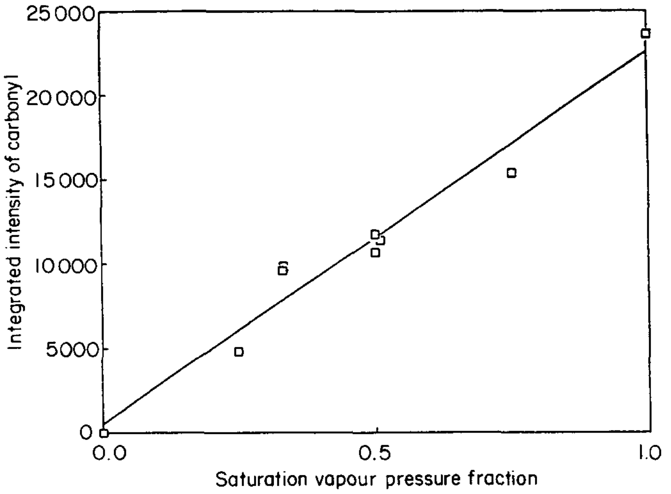

Figure 3 Calibration curve. Integrated intensity of EtAc obtained from the photoacoustic *FT*i.r. experiment plotted as a function of saturation vapour pressure of EtAc in the cell

cell without application of strain and photoacoustically monitoring EtAc diffusion as a function of time. Between each spectral collection, the cell was purged for 30 s with helium. As a result, the diffusion time axis on the plots of RPA *FT*i.r. intensity represents the difference between removal of the film from the EtAc and the collection of 200 scans (half the number of total scans for each spectrum).

In the second series of experiments, the initial RPA *FT*i.r. spectra were also collected at 0% elongation, followed by subsequent spectral collections after the sample was elongated in increments of 0.83% or 1.7%. In a typical experiment, each strain – measurement cycle consisted of elongating the sample, purging the cell compartment for 30 s with helium, and collecting the spectra. The film was narrowed by ~50% in a centre film area to control the location of neck formation. In order to follow the effect of elastic strain on non-plastically deformed regions of the film, the neck was purposely allowed to form outside the cell.

In an effort to determine the effect of plastic transformations on transport properties, the third series of experiments involved the neck formation in the RPA *FT*i.r. cell. The integrated intensity of the 1768 cm^{-1} band attributed to the carbonyl band of EtAc was used to determine the amount of EtAc present. For that reason, the calibration curve shown in *Figure 3*, which relates the integrated intensity to EtAc vapour concentration in the cell, was determined by injecting a known concentration of EtAc vapour into the cell, followed by collection of the photoacoustic *FT*i.r. spectra. It should be noted that the 1768 cm^{-1} band is attributed to EtAc vapour. The band due to the same carbonyl normal vibrations in liquid EtAc would be detected at lower vibrational energies due to extensive hydrogen bonding in the liquid phase.

In order to establish mechanical characteristics of PVF_2, stress–strain experiments were independently performed on an Instron mechanical tester. Film dimensions were the same as those used in the RPA *FT*i.r. spectroscopic studies. PVF_2 films unexposed to EtAc and films saturated with EtAc were drawn at a rate of 5% min^{-1} to an elongation of 14%. This elongation was sufficient to induce neck formation.

X-ray diffraction studies were performed on films as received, and on neck regions of drawn samples which had undergone local elongations of 450% or more. Such local elongations lead to α–β phase transformation in PVF_2. All diffractograms were collected on a Philips diffractometer using a long Cu fine-focus tube operated at 45 kV and 30 mA. The samples were scanned over the 2θ range of 2–50, with a step of 0.025 and 1 s collection intervals.

RESULTS AND DISCUSSION

As a first step in the analysis of gas phase EtAc molecules diffusing out of PVF_2, it is important to establish the initial concentration of these species in the polymer. Because the simplest approach is to saturate PVF_2 with EtAc and use that as a basis for further analysis, let us determine the time required to saturate PVF_2 with EtAc. The concentration of EtAc can be monitored by following the intensity changes of the carbonyl normal vibration at 1768 cm^{-1} of EtAc in the gas phase. This is plotted in *Figure 4* as a function of time. Each data point of the overlapping curves in *Figure 4* represents the integrated intensity of the carbonyl band of EtAc which was given off during the 7 min period required to collect each 400-scan spectrum. Curves A and B were obtained for PVF_2 films soaked in EtAc for 40 h and 1 month, respectively. The decreasing rate of EtAc loss over the course of the experiment is the same for both films, indicating that 40 h is a sufficient length of time for the saturation of PVF_2 with EtAc. The initial rapid decay of EtAc concentration in the vapour phase is attributed to two major factors; the most pronounced one is that the amount of EtAc in the film decreases with time, and therefore, less EtAc is available for evaporation in the later stages. Furthermore, since the diffusant adds to the free volume, and D is therefore dependent upon the EtAc concentration[6], the initial decrease of the sorbate concentration in the film leads to a decrease of D. Apparently, D decreases rapidly during the early stages of the experiment and, as the EtAc concentration quickly diminishes, it levels off in the later stages. As the rate at which EtAc is being eluted from the film decreases, the rate at which D changes, also decreases. The diffusion

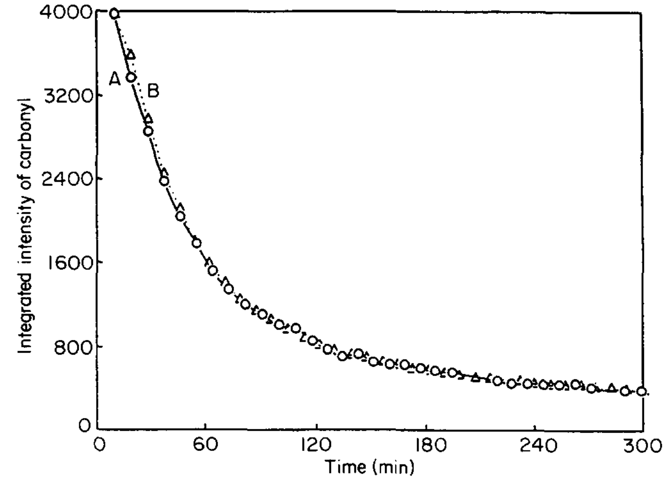

Figure 4 Integrated intensity of the carbonyl band at 1768 cm^{-1} plotted as a function of time for films soaked in EtAc for (A) 40 h and (B) 1 month

rate changes will be discussed and analysed quantitatively in future publications[16].

As indicated in the Introduction, in an effort to determine the effect of elastic and plastic elongations on the transport properties of EtAc in PVF$_2$, the samples should be elongated. The strain measurements are reported as a total amount of strain the entire sample has experienced, but because PVF$_2$ elongates with 'neck' formation, this feature should be taken into account. During the first few per cent elongation, the film elongates uniformly. Following the yield point, however, all additional elongation contributes to neck formation in the central regions of the film. As noted in the literature[1], plastic deformation occurs only in the region of neck formation, whereas all deformation outside the neck is considered to be elastic. In an effort to monitor the effect of FFV changes on D and to eliminate the possibility of interference caused by the strong D dependence upon concentration in the early stages of evaporation, films saturated with EtAc were dried for a certain time before the elongation experiments were conducted. Because the primary focus of this study is to correlate the structure of PVF$_2$ with transport properties, there are two regions in the PVF$_2$ films which will be considered; the region that undergoes transformation from α to β crystalline form and the one that maintains its original α form[9].

Effect of elastic strain on the transport properties

Similarly to the results presented in *Figure 4*, *Figure 5* illustrates the changes in the 1768 cm^{-1} band due to gaseous EtAc, but now plotted as a function of PVF$_2$ film elongation. The effect of elastic deformation on the transport properties can be monitored by analysis of the neck formed outside the RPA *FT*i.r. cell. Curves A–D represent the integrated intensities of the carbonyl band for the samples dried for various lengths of time before recording the initial RPA *FT*i.r. spectra. These data indicate that initially the concentration of EtAc in the vapour phase increases, followed by a steady decrease. For 30 and 60 min drying times, curves A and B exhibit a maximum diffusion at 1.7% elongation. This behaviour is attributed to the increased FFV of the film, created by elongation that allows EtAc to diffuse out of the film at faster rates. However, curves C and D do not reach a maximum until 4.2% strain. This is because there is an EtAc concentration difference at the beginning of each experiment. As illustrated in *Figure 5* for 0% elongation, longer drying times give lower initial EtAc concentrations. The initial increase of FFV results in an increased rate of diffusion. If the film was not dried for a sufficient period of time, the concentration of EtAc in the vapour phase would achieve a maximum after 1.7% strain. This maximum cannot be maintained because of the rapidly decreasing concentration of EtAc in the film. After the films have been allowed to dry beyond the period of rapid changes in EtAc concentration, as illustrated by curves C and D in *Figure 5*, if the FFV remains unchanged, the amount of EtAc entering the vapour phase should decrease due to the decreasing EtAc concentration. Thus, the free volume changes appear to cease at 4.2% elongation in the regions of the polymer that do not undergo neck formation. This is attributed to the increase of FFV, which affects the rate of diffusion in this elongation range, because the intensity of the carbonyl band will increase as long as the FFV continues to increase.

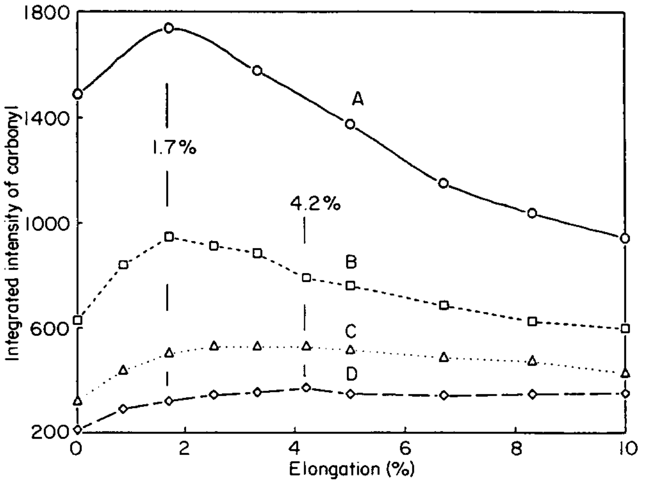

Figure 5 Integrated intensity of the carbonyl band at 1768 cm^{-1} plotted as a function of elongation. Curves A, B, C and D represent films dried 30, 60, 120 and 240 min prior to elongation, respectively

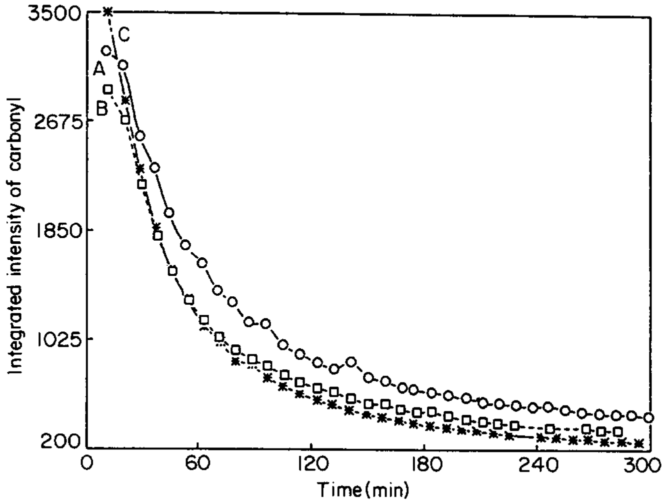

Figure 6 Intensity of the carbonyl band at 1768 cm^{-1} plotted as a function of time. Curve A was obtained using a film as received. Curves B and C were obtained from films strained 1.7 and 5%, respectively

The effect of elastic strain was also examined by determining the EtAc loss from PVF$_2$ which had experienced elongations of 5% or less. *Figure 6* illustrates the integrated intensity of the 1768 cm^{-1} band plotted as a function of time (see Experimental section for details). Curve A represents a non-strained film, whereas curves B and C illustrate the rate of loss of EtAc from the films elongated 1.7 and 5%, respectively. It appears that for the non-strained polymer (curve A), the rate at which EtAc diffuses is slower, indicating that the strain applied to the films enhances the rate of diffusion of EtAc, such as that illustrated by curves B and C.

If elongation of a polymer increases its FFV, spectroscopic analysis of the EtAc vapour above the PVF$_2$ films saturated with EtAc and strained 1.7 and 5% should be reflected in the EtAc concentration changes in the gas phase. Such an approach will allow the monitoring of EtAc diffusing off the films that have different FFV contents. The analysis of *Figure 6* indicates that the films strained 5% lose EtAc at a faster rate than the samples with no or 1.7% elongation. This behaviour is expected because the increase of FFV is proportional to the extent of strain[3]. Therefore, the film with the highest concentration of EtAc in the vapour phase in the early stages of the experiment has the lowest concentration in the later stages. This results from the enhanced transport properties upon elongation.

Effect of plastic strain on transport properties

The yield point marks the point at which elastic deformation reaches its maximum and beyond which the applied strain results in plastic deformations. In an effort to establish the point at which plastic strain occurs, the stress–strain behaviour of PVF$_2$ was examined using an Instron instrument. The results are shown in *Figure 7*. Curve A represents the results obtained for the polymer free of EtAc, whereas curve B is that of PVF$_2$ saturated with EtAc. It is apparent that both curves initially increase, reaching maxima, followed by decay and subsequent levelling off. The onset of void formation in the neck region, identified by changes in appearance from transparent to white in the narrowed region of the film, is marked on the curves in *Figure 7*. Unswollen PVF$_2$ (curve A) experiences a higher stress, whereas EtAc saturated PVF$_2$ (curve B) yields at lower stress levels. This behaviour is attributed to the plasticizing effect of EtAc which aids the polymer chains in sliding past one another, and results in a smaller build up of stresses required to induce plastic deformation in the swollen state. Although the polymer is elongated ~14%, a fraction in the neck region has undergone an elongation of 450% or more, and this elongation is sufficient to ensure a large degree of transformation to a fibrillar morphology[1], resulting in the crystallinity changes[9]. In an effort to identify the changes in crystalline polymer structures occurring during neck formation, X-ray diffraction measurements were performed. The X-ray data presented in *Figure 8* indicate a large scale molecular level restructuring. The diffractogram of the unstretched polymer (trace A) contains several sharp peaks indicating crystallinity on a background created by scattering from the amorphous regions of the polymer. These observations suggest that the unstretched film consists of well defined crystalline regions, randomly oriented in an amorphous phase. Although trace B of *Figure 8* is dominated by one strong peak due to the β phase, its breadth indicates that the crystal structure is not well defined. The peak intensities, and the lower background scattering attributed to the amorphous phase, indicate a greater overall order of the drawn PVF$_2$ film. This observation suggests that the crystallites as well as the amorphous phase between them are oriented parallel to the direction of elongation, as predicated by the fibrillar structure model[1,7]. The X-ray diffraction studies are thus consistent with our proposed explanation for the variable rate of diffusion of EtAc in PVF$_2$, in that diffusion is slowed down through more ordered structures such as those found in fibrous polymers.

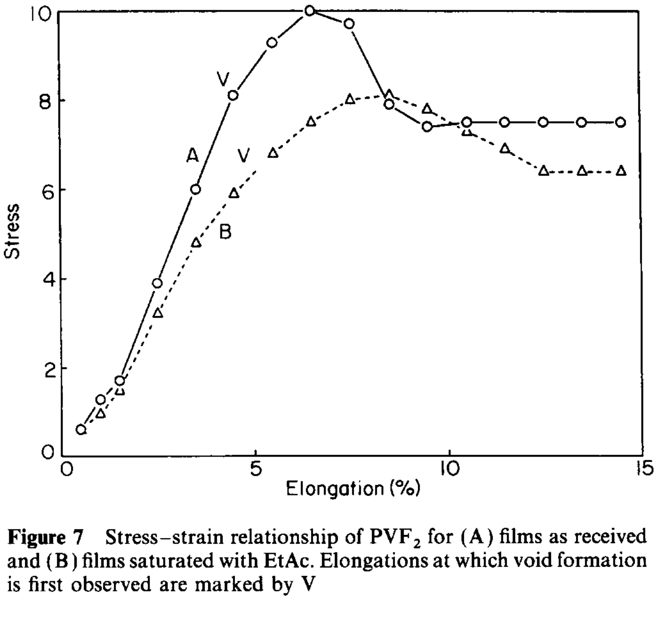

Figure 7 Stress–strain relationship of PVF$_2$ for (A) films as received and (B) films saturated with EtAc. Elongations at which void formation is first observed are marked by V

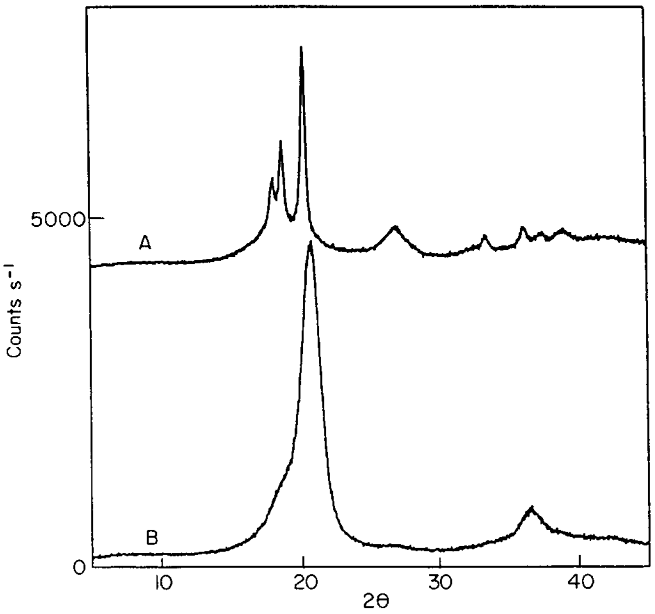

Figure 8 X-ray diffractograms of PVF$_2$ (A) as received and (B) the neck region of a drawn film

In light of the previous considerations, it is apparent that the primary changes in the polymer morphology occur as a result of plastic strain which, in turn, may affect the polymer transport properties. This effect was examined by straining the films with the neck forming in the i.r. beam, but the spectra were collected on the films not covered with the photoacoustic umbrella. *Figure 9* illustrates a series of plots with the intensity of the carbonyl band of EtAc at 1768 cm^{-1} plotted as a function of elongation. Curves A–D represent the data for PVF$_2$ films dried for 15, 30, 60 and 150 min prior to spectroscopic analysis. It is quite apparent that there is a much faster increase in the diffusion rate resulting from plastic deformation than that observed for elastic deformations presented in *Figure 5*. Because the films were not covered with the photoacoustic umbrella during the measurements, the plots shown in *Figure 9* represent contributions from EtAc in the polymer as well as from gaseous EtAc in the cell. With progressively longer drying times, the intensity of the carbonyl band at 0% elongation decreases, indicating a smaller initial concentration of EtAc.

The data depicted in *Figure 9* represent the change in transport properties that occur in the region of the polymer undergoing plastic deformation. The increase of EtAc exudating during the first few per cent of elongation before the neck is being formed is again attributed to the opening of the spherulitic structures and the subsequent

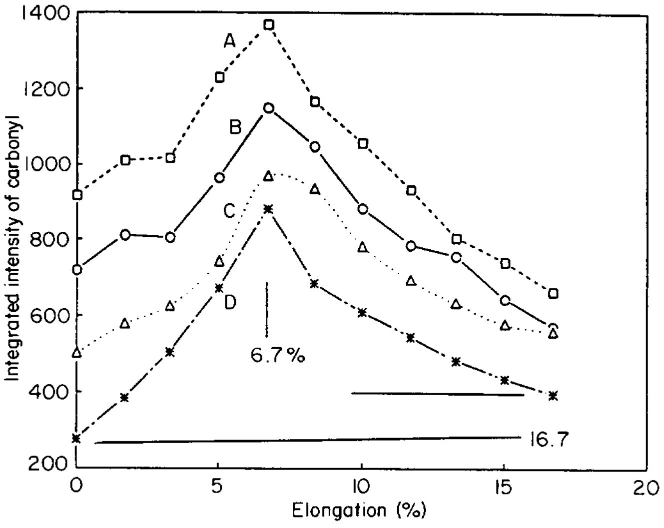

Figure 9 Integrated intensity of the carbonyl band at 1768 cm^{-1} plotted as a function of elongation. Data obtained without shielding the PVF$_2$ from the i.r. beam. Curves A, B, C and D represent films dried 15, 30, 60 and 150 min, respectively

increase of FFV. The above assessments are in agreement with the data presented in *Figure 5*, indicating that the strain increase leads to the increased FFV. Furthermore, the data presented in *Figure 5* indicate that above 4.2% strain, the FFV changes in the regions not undergoing neck formation. These observations suggest that above this elongation level, all subsequent deformations, up to the neck formation, occur in the film region narrowed by 50%, because further elongation in the non-necking regions would increase their FFV. Elongations up to 5% result in a whitening of the film as voids are formed between the spherulites. When elongation reaches 6.7% (*Figure 9*), completion of void formation in the regions of the film that form the initial neck is achieved. The voids provide unobstructed diffusion pathways, greatly enhancing the transport properties of the film. Thus, the increasing intensity of the band at 1768 cm^{-1} due to EtAc in the gas phase is attributed to the opening of the spherulitic structures which, in turn, increases FFV and ends with void formation. The location of the maximum for each curve suggests that the permeability of the films reaches a maximum at 6.7% elongation. Further strain induces no change in the polymer morphology which could possibly further increase the rate of diffusion, making the amount of EtAc leaving the film dependent upon the EtAc concentration in the polymer. Although one could speculate that the maximum at 6.7% could be solely due to the decreasing EtAc concentration in the sample, the experiments were performed over a wide range of EtAc concentrations, and that would reveal any concentration effect on the maxima location. Furthermore, the sensitivity of photoacoustic *FT*i.r. to gas phase analysis has been known to be as high as parts per billion.

A substantial increase of the transport properties with void formation is demonstrated by curve D in *Figure 9*. After the film has been dried for 150 min, this length of time is beyond the range of rapid diffusion rate changes. The amount of EtAc in the cell during the spectrum collection at 16.7% elongation is larger than the amount diffusing out of the film during the collection of the first spectrum. This phenomenon occurs despite the lower concentration of EtAc in the polymer at the end of the experiment and suggests that the enhancement of transport properties results from the presence of voids in the film.

The data presented in *Figure 10* show the intensity changes of the carbonyl band at 1768 cm^{-1} due to EtAc above covered PVF$_2$ film as a function of the film elongation. However, in this experiment, curves A, B and C represent drying times of 20, 60 and 120 min, respectively, and indicate that the longer drying times result in higher elongations at which the maximum of EtAc in the gas phase is reached. The location of the maximum of the EtAc vapour intensity depends upon the initial concentration of EtAc. This is illustrated in *Figure 10*, where the polymer from which curve A was derived experienced an increased diffusion rate attributed to the opening of the spherulitic structures resulting from 3.3% elongation. Curves B and C were obtained from the RPA *FT*i.r. experiments on the films with lower EtAc concentrations at the beginning of the experiments.

Curves A of *Figures 5* and *10* represent the analysis of EtAc diffusion from the polymer being exposed to the same drying period and conditions. In contrast to the results presented in *Figure 5*, the data illustrated in *Figure 10* were obtained over the forming neck. The greater intensity change of curve A in *Figure 10* suggests that even before the onset of neck formation, the narrowed region of the polymer undergoes a larger local strain. This behaviour is expected since a narrower region of the film would experience a higher degree of stress per unit cross-sectional area.

In an effort to relate macroscopic changes occurring during the course of the experiment to spectroscopic data, it was realized that upon film elongation, the rate at which EtAc diffuses out of the film changes. This observation is attributed to the spherulitic to fibrillar morphology changes, which affect the rate of EtAc loss from a PVF$_2$ film. *Figure 11* demonstrates the relative rate loss of EtAc from PVF$_2$ in its original spherulitic and fibrous neck forms. Curve A represents the rate of loss from the spherulitic stress-free film, whereas curves B and C are the rate of EtAc loss from the neck regions of the films. In both cases, the stretched films were re-saturated with EtAc. Curve C was obtained from the film subjected to a constant stress during the spectral collection. In the fibrous structure (*Figure 11*, curve B),

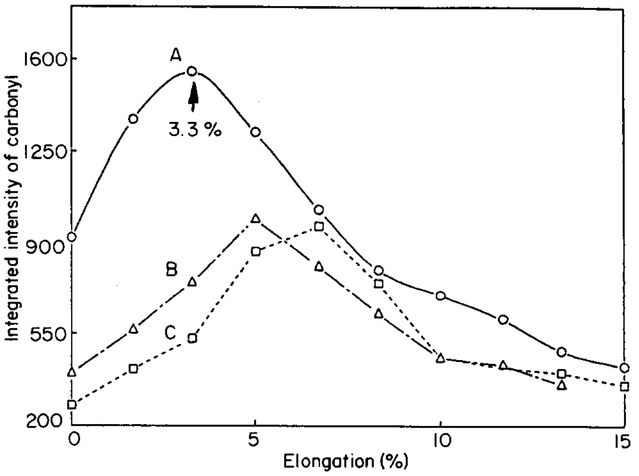

Figure 10 Integrated intensity of the carbonyl band at 1768 cm^{-1} plotted as a function of elongation. Data acquired with PVF$_2$ film shielded from the i.r. beam. Curves A, B and C represent films dried 20, 60 and 120 min, respectively

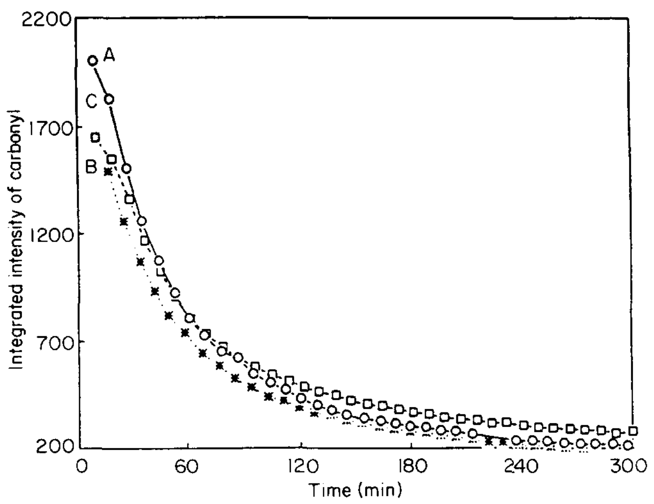

Figure 11 Integrated intensity of the carbonyl band at 1768 cm^{-1} plotted as a function of time for: (A) non-strained films; (B) stress relaxed neck regions of prestrained and re-saturated films; (C) films prestrained, re-saturated and monitored while strained 1.7%

the amorphous component is more ordered, resulting in a lower FFV, a higher activation energy of diffusion, and a smaller D (refs 17 and 18). This is demonstrated by a slower decrease in the gas phase intensity for fibrous PVF$_2$ (curve B) as compared to the spherulitic structure (curve A).

When prestretched films are immersed in EtAc, the whiteness, attributed to the presence of voids in the neck region[1], disappears. This observation indicates that the plasticizing effect of EtAc allows the polymer chains to relax, leading to void elimination. As shown in *Figure 11*, a comparison of curves B and C suggests that the diffusion of EtAc is reduced upon application of stress to fibrous films. This is again demonstrated by the relative rate decrease of the EtAc carbonyl band at 1768 cm^{-1}. This difference in the intensity changes, which is related to the rate of diffusion, is believed to be due to the relaxation of the tie molecules between crystallites in the presence of EtAc, when the fibrous films are saturated with EtAc. The presence of EtAc enables relaxation of the internal stresses and enhances the freedom of motion of the polymer chains in amorphous regions. When strain is applied, the amorphous regions are compressed by the tie molecules and transport is reduced.

Up to this point, a qualitative description for the diffusion rates in PVF$_2$ films with different morphologies has been discussed. However, a semiquantitative treatment of the data may yield not only information about the diffusion rates but further information about the changes of polymer morphology. For that reason, the integrated intensity of the i.r. band at 1768 cm^{-1} was used to determine the concentration of EtAc vapour in the photoacoustic *FT*i.r. cell. It should be realized that this analysis holds only for gas phase EtAc where there is no hydrogen bonding between the EtAc molecules. It cannot be applied when EtAc molecules are in the liquid phase, where extensive hydrogen bonding may cause the 1768 cm^{-1} band to shift to as low as 1720 cm^{-1}. As demonstrated in *Figure 3*, the intensity of the photoacoustic signal of an organic vapour is proportional to the vapour pressure in the cell. Knowing the saturation vapour pressure[19], and the volume of the cell, the measurement of the photoacoustic signal at various vapour pressures in the cell enables us to correlate the RPA *FT*i.r. integrated intensity of the carbonyl band to the amount of vapour present. The integrated intensity of the band at 1768 cm^{-1} is proportional to the amount of vapour inside the cell through the following relationship:

$$C = PA \times (2.03 \times 10^{-8}\ \mathrm{g\ cm^{-3}}) \qquad (2)$$

where C is the concentration of EtAc and PA is the

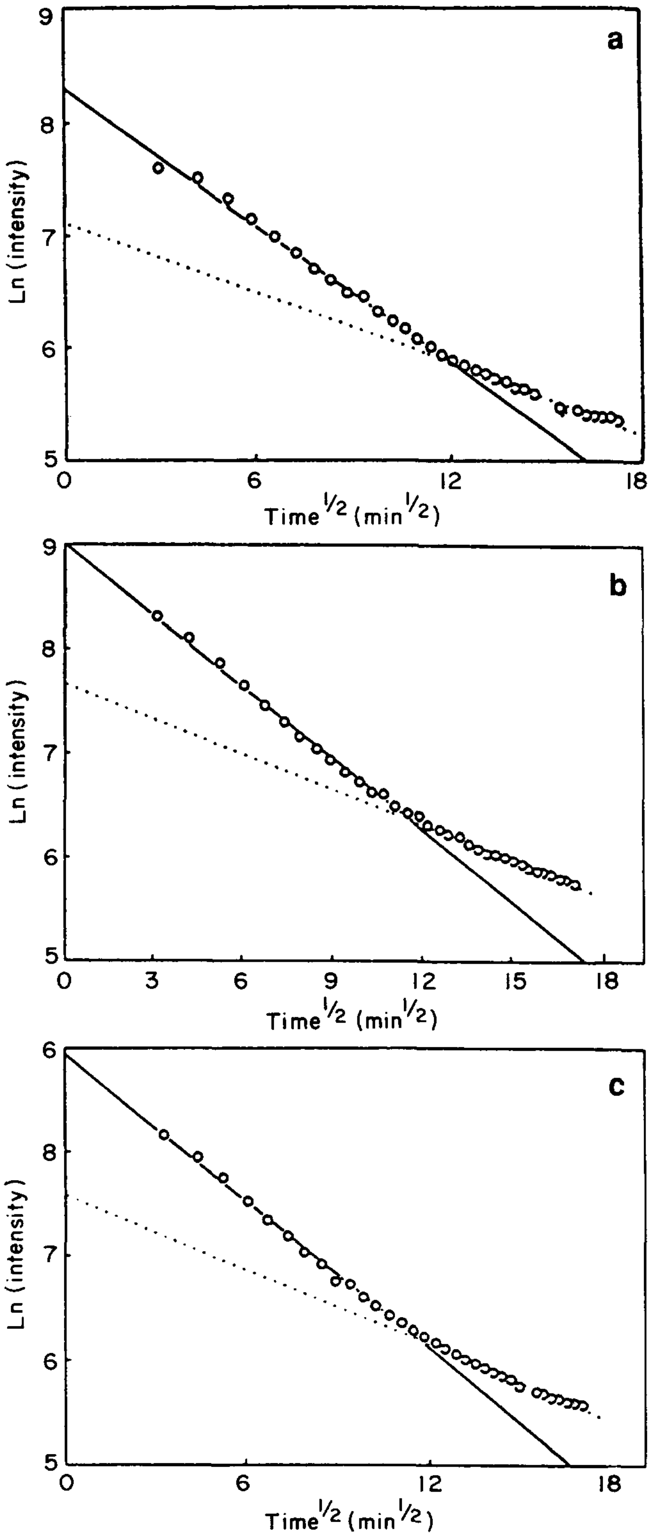

Figure 12 Natural logarithm of the integrated intensity of the carbonyl band at 1768 cm^{-1} plotted *versus* the square root of time at which the spectra were collected. Films: (a) as received; (b) strained 1.7%; (c) strained 5%

Table 1 Exponents and pre-exponential values obtained for equation (3) from PVF$_2$ under the conditions listed in the Experimental section

	Diffusion time			
	0–140 min		140–300 min	
PVF$_2$ sample	x[a]	ln A[b]	x	ln A
Spherulitic form				
0% elongation	0.198	8.70	0.105	7.60
1.7% elongation	0.214	8.86	0.108	7.60
5% elongation	0.232	8.99	0.122	7.73
Fibrous form				
0% elongation	0.168	8.09	0.099	7.26
1.7% elongation	0.167	8.02	0.087	7.09

[a] Exponent in equation (3)
[b] Intercept of the integrated intensity axis at time = 0

integrated intensity of the carbonyl band. It has been recognized for a long time that the rate of diffusion of small molecules in many polymers is exponentially related to the diffusant concentration[6]. Assuming that the plots in *Figure 4*, *6* and *11* follow the relation:

$$PA = A\exp[x(-t^{1/2})] \qquad (3)$$

the natural log of the intensity plotted as a function of the square root of time will result in a slope equal to x, a parameter dependent upon the film morphology. In equation (3), A is a pre-exponential term representing the log of the integrated photoacoustic *FT*i.r. intensity at $t = 0$.

Applying equation (3) to curves A, B and C in *Figure 6* results in the plots presented in *Figure 12*. The slopes of the lines provide the value of x, which is proportional to the desorption diffusion coefficient[16]. The values of x obtained for stressed and non-stressed PVF$_2$ are listed in *Table 1*. It is apparent from the data in *Table 1* that the application of stress increases the rate of diffusion from the PVF$_2$ films in spherulitic form. This is illustrated by the higher x values for the strained films. In constrast, stress decreases the rate of diffusion from films with a fibrillar structure, as demonstrated by the low x value for strained fibrous PVF$_2$.

CONCLUSIONS

In this work the utility of the newly developed RPA *FT*i.r. spectroscopy method has been demonstrated for measuring the rate of diffusion of organic molecules from polymeric matrices. The analysis of spectroscopic data allows a comparison of the diffusion rate from PVF$_2$ under various conditions. These studies show that the diffusion rates of EtAc in PVF$_2$ are lower in films having a fibrous structure. The application of stress increases the transport of EtAc in spherulitic PVF$_2$ and leads to its decrease for fibrillar structures. The morphological changes occurring in plastic deformation increase the diffusion rate to a greater extent than the deformations of elastic strain.

ACKNOWLEDGEMENTS

The authors are grateful to 3M Company, St Paul, MN, USA for partial support of this work.

REFERENCES

1 Hsu, T. C. and Geil, P. H. *J. Mater. Sci.* 1989, **24**, 121
2 Phillips, J. C. and Peterlin, A. *Polym. Eng. Sci.* 1983, **23**, 734
3 Peterlin, A. *J. Macromol. Sci.* 1975, **B11**, 57
4 Yasuda, H., Stannet, V., Frisch, H. L. and Peterlin, A. *Makromol. Chem.* 1964, **73**, 188
5 Peterlin, A. and McCrackin, F. L. *J. Polym. Sci., Polym. Phys. Edn* 1981, **19**, 1103
6 Vittoria, V., DeCandia, F., Capodano, V. and Peterlin, A. *J. Polym. Sci., Polym. Phys. Edn* 1986, **24**, 1009
7 Meares, P. *Eur. Polym. J.* 1966, **2**, 95
8 Phillips, J. C., Peterlin, A. and Waters, P. F. *Polym. Mater. Sci. Eng.* 1983, **49**, 555
9 Siesler, H. W. *J. Polym. Sci., Polym. Phys. Edn* 1985, **23**, 2413
10 Matsushige, K. and Takemura, T. *J. Polym. Sci., Polym. Phys. Edn* 1978, **16**, 921
11 McDonald, W. F., Goettler, H. and Urban, M. W. *Appl. Spectrosc.* 1989, **43**, 1387
12 Urban, M. W., McDonald, W. F., Gaboury, S. and Tiefenthaler, A. in 'Polymer Characterization' (Eds C. D. Craver and T. Provder), American Chemical Society, Washington DC, 1990
13 Phillips, J. C., Peterlin, A. and Waters, P. F. *J. Polym. Sci., Polym. Phys. Edn* 1981, **19**, 789
14 McDonald, W. F. and Urban, M. W. *Adhes. Sci. Technol.* 1990, **4**, 751
15 Huang, J. B. and Urban, M. W. unpublished results
16 Ludwig, B. W. and Urban, M. W. *Polymer* submitted
17 Peterlin, A., Williams, J. L. and Stannett, V. *J. Polym. Sci. A2* 1967, **5**, 957
18 Williams, J. L. and Peterlin, A. *J. Polym. Sci. A2* 1971, **9**, 1483
19 Dreisbach, R. R. 'P–V–T Relationships of Organic Compounds', Handbook Publishers, Sandusky, 1952